New Journal of Physics
The open access journal at the forefront of physics

Deutsche Physikalische Gesellschaft DPG IOP Institute of Physics

PAPER • OPEN ACCESS

# Wave function engineering in quantum dot–ring nanostructures

To cite this article: Elbieta Zipper *et al* 2012 *New J. Phys.* **14** 093029

New Journal of Physics
The open-access journal for physics

# Wave function engineering in quantum dot–ring nanostructures

**Elżbieta Zipper, Marcin Kurpas and Maciej M Maśka**[1]
Institute of Physics, University of Silesia, ul Uniwersytecka 4,
40-007 Katowice, Poland
E-mail: maciej.maska@us.edu.pl

*New Journal of Physics* **14** (2012) 093029 (16pp)
Received 16 May 2012
Published 17 September 2012
Online at http://www.njp.org/
doi:10.1088/1367-2630/14/9/093029

**Abstract.** Modern nanotechnology allows the production of, depending on the application, various quantum nanostructures with selected properties. These properties are strongly influenced by the confinement potential which can be modified e.g. by electrical gating. In this paper, we analyze a nanostructure composed of a quantum dot surrounded by a quantum ring. We show that, depending on the details of the confining potential, the electron wave functions can be located in different parts of the structure. Since many properties of such a nanostructure strongly depend on the distribution of the wave functions, by varying the applied gate voltage one can easily control them. In particular, we illustrate the high controllability of the nanostructure by demonstrating how its coherent, optical and conducting properties can be drastically changed by a small modification of the confining potential.

[1] Author to whom any correspondence should be addressed.

## Contents



## 1. Introduction

Wave function engineering refers to an unprecedented ability to adjust the spatial distribution of the electron wave function in quantum nanostructures through the control of their growth, geometry and electrical fields. It allows us to explore the basic issues of quantum mechanics to design new devices in which some specific properties can be optimized.

Nanotechnology [1, 2] now enables precise control of structural parameters both at the fabrication stage of quantum nanostructures [3, 4] as well as dynamically while operating the device, e.g. through the electrostatic potential [5]. Recent progress allows us to produce complex systems where different building blocks, such as quantum dots (QDs) [6, 7] and quantum rings (QRs) [8], are combined together within a single structure. Such quantum structures are highly relevant to new technologies in which the control and manipulation of electron spin and wave functions play an important role [9]. The potential use of such devices requires, however, deep theoretical analysis.

We have looked for a complex system composed of coupled elements where the coupling constant is an additional parameter that can be controlled by electrical gating. The electronic properties of such a structure can be fine-tuned, which allows monitoring of its properties. In this context, we have performed a comprehensive theoretical analysis of a two-dimensional nanostructure in the form of a QD surrounded by a QR, named afterwards a dot–ring nanostructure (DRN). Such a structure has recently been fabricated by droplet epitaxy [3]. We show that by changing the confinement potential, i.e. the parameters of the potential barrier $V_0(r)$ separating the dot from the ring and/or the potential well offset $V_{QD}-V_{QR}$ (see figure 1), one can considerably alter its optical, conducting and coherent properties.

In particular, we show that by such manipulations one can change:

(a) the spin relaxation time $T_1$ of DRNs, used as spin qubits or spin memory devices, by orders of magnitude,
(b) the cross section for frequency selective optical absorption at the microwave and infrared range from strong to negligible,
(c) the conducting properties of an array of DRNs from highly conducting to insulating.

These features are mostly determined by the so-called overlap factor (OF) (given by equation (3)), which reflects the shape and distribution of the wave functions and can be largely

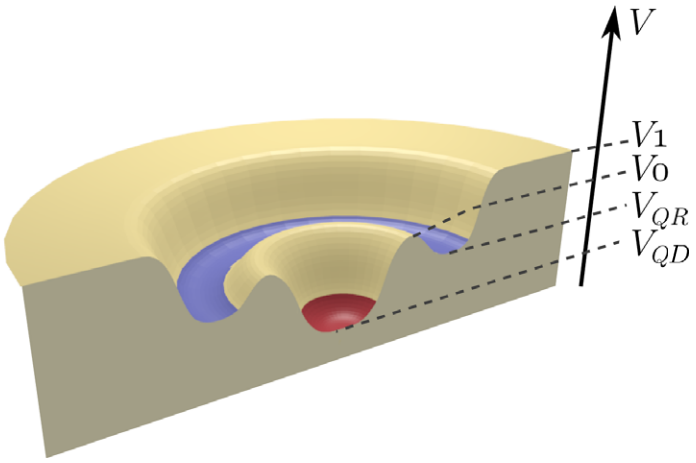


**Figure 1.** Cross section of the confining potential of a DRN with the marked bottom of the QD potential ($V_{\mathrm{QD}}$), the bottom of the QR potential ($V_{\mathrm{QR}}$), the height of the barrier potential ($V_0$) and the value of the potential outside the DRN ($V_1$). We set $V_{\mathrm{QR}} = 0$. The actual cross sections of the potentials used in calculations are shown in figures 4, 6 and 8.

modified by the form of the confinement potential. Thus the microscopic properties of a DRN can be engineered on demand, depending on a particular application.

The paper is organized as follows. In section 2 we present a general theoretical background that will be needed to study particular properties of DRNs. In the following sections we demonstrate, by changing the parameters of the confinement potential, that we can control the spin relaxation time (section 3), the optical absorption (section 4) and the transport properties of DRNs (section 5). The results are summarized in section 6.

## 2. Basic theoretical formulae

We consider a two-dimensional, circularly symmetric DRN defined by a confinement potential $V(r)$. The DRN is composed of a QD surrounded by a QR and separated from the ring by a potential barrier $V_0$. We assume that the barrier is sufficiently small to allow electron tunnelling between the QD and QR. It ensures that if we change the confining potential at low temperature the electron always occupies the ground state independently of the previous shape of the potential. A cross section of a DRN with explanations of symbols used throughout the text is presented in figure 1.

Such a confinement potential, which conserves the circular symmetry, can be obtained in many ways [1, 10]. Electrostatically defined DRNs can be fabricated, e.g. within a two-dimensional electron gas by placing two gates on the top of it [11, 12]. The gates should have a form of a central circular gate surrounded by a collar gate. The electrons are confined in the quantum well in the regions below the split gates. They can also be constructed by first producing the QD in the two-dimensional electron gas and then performing local oxidation of a narrow circular strip inside it with an atomic force microscope [13]. The electron gas is depleted below the oxidized region thus splitting the structure into the QR with the QD inside. Another method is via droplet epitaxy [3, 14]. The growth procedure is based on the pulsed irradiation of group-V element to group-III element nanoscale droplets at a controlled temperature and

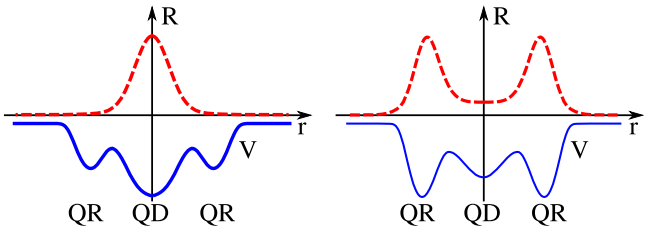


**Figure 2.** Schematic illustration of the radial part $R$ of the ground state wave function in the case where the QD potential is deeper than the QR potential (left panel) or vice versa (right panel). The solid blue line represents a cross section of the confining potential obtained from the Laplace equation, whereas the dashed red line is a solution of the corresponding Schrödinger equation.

fluxes for transforming them into various nanostructures. Droplet epitaxy growth of GaAs allows, through the fine control of As flux and substrate temperature, production of quantum nanostructures with the desired shape, size and dimensionality. It permits combination of QDs and QRs into a single, multifunctional nanostructure, in particular the central QD surrounded by one or more concentric QRs. The discussed structures may also be created by lithography [1, 2].

We start with the confining potential produced solely by electrostatic gating. The electrostatic definition allows one to control and alter the entire potential landscape. In order to make our theoretical results more realistic, the shape of the confinement potential is found by solving the Laplace equation[2]. Unfortunately, the electrostatically defined nanostructures are relatively large and therefore the resulting relaxation times are small. However, by applying voltage to electrodes one is able to modify the confining potential also in nanostructures produced by means of other methods. In such a case the size of the DRN can be much smaller and we will show that then the relaxation times can be much larger. In order to do that we will assume a smooth confining potential similar to that found from the Laplace equation, but of a smaller diameter.

The most important feature of a DRN is the controllability of the shape of the electron wave functions. The main parameters that affect this shape are the relative positions of the bottoms of the QD and QR confining potentials and the size of the barrier between them. These parameters can be tuned, e.g. by electrical gating. Roughly speaking, if the potential of the QD is much deeper than the potential of the QR, the electrons are located mainly in the QD and the effective size of the wave function is small. On the other hand, if the ring's potential is much deeper the electrons occupy only states in the QR and the wave function is much broader (figure 2). Moreover, by fine-tuning the confinement potential we are able to have, e.g. the ground state located in the QD, with the lowest excited state in the QR (or vice versa). This way we can easily control the OF and all the properties which depend on it. In sections 3 and 4, we show how this feature can be exploited to control relaxation time and optical absorption.

As it was already stated, the confinement potential of the required shape can be produced in many ways. We start with an example of a DRN electrostatically defined by two planar concentric electrodes, a circular one in the center surrounded by a ring-shaped electrode. For such a system we solve the Laplace equations. Depending on the parameters (dimensions and voltages) the resulting potential may smoothly evolve between the limits presented in

[2] The authors are grateful to Bartłomiej Szafran and Michał Nowak for providing the code that was used in this calculation.

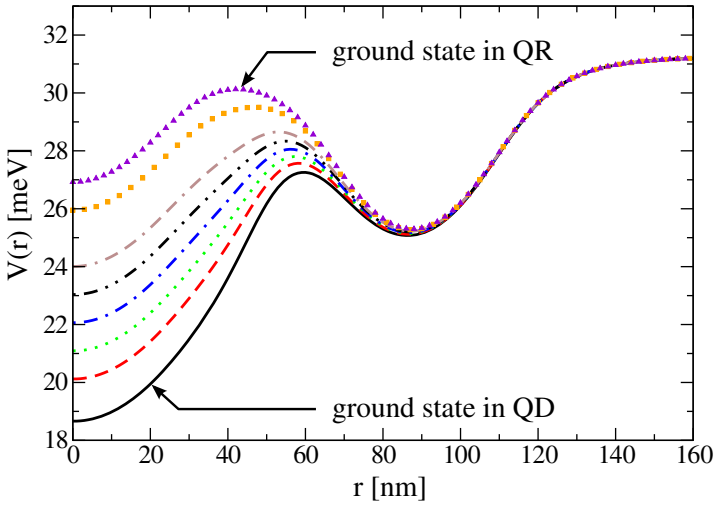


**Figure 3.** Cross section of the confining potential for different voltages applied to the electrodes.

figure 2. Figure 3 demonstrates the evolution of the potential when the voltage applied to the electrodes is varied. Since our analyses are not limited to electrostatically defined DRNs in calculations we will use a smooth general confining potential of the form proposed in [15, 16]. This potential can be very well fitted to the solution of the Laplace equation, but can describe smaller nanostructures as well. It is important for our analysis that such a potential allows us to study independently the influence of the height of the barrier and the relative position of the bottoms of the potentials of the QR and QD (see figures 4, 6 and 8). In numerical calculations we assume the size of the DRN to be equal to about 160 nm, $V_1 = 50$ meV and we set the zero potential energy at the level of $V_{\mathrm{QR}}$, i.e. the potential well offset is equal to $V_{\mathrm{QD}}$. To be specific, our model calculations are performed for InGaAs systems (with the effective electron mass $m^* = 0.067 m_{\mathrm{e}}$ and the electron spin $g$-factor $|g_{\mathrm{s}}| = 0.8$) for which many theoretical and experimental investigations have been done.

The single-electron Hamiltonian with the confinement potential $V(r)$ and in the presence of the in-plane magnetic field $B$ is written as

$$H = \frac{1}{2m^*}\mathbf{p}^2 + \frac{e\hbar}{2m^*}\hat{\sigma}\cdot\mathbf{B} + V(r). \tag{1}$$

The energy spectrum of $H$ consists of a set of discrete states $E_{nl}$ due to radial motion with radial quantum numbers $n = 0, 1, 2, \ldots$, and rotational motion with angular momentum quantum numbers $l = 0, \pm 1, \pm 2 \ldots$. The single-particle wave function is of the form

$$\Psi_{nl\sigma} = R_{nl}(r)\exp(\mathrm{i}\, l\phi)\,\chi_\sigma, \tag{2}$$

with the radial part $R_{nl}(r)$ and the spin part $\chi_\sigma$.

For many QDs the energy spectra and the wave functions can be calculated analytically, for other structures have to be calculated numerically. Having given the wave functions one can calculate the OF. It reflects the mutual distribution of the radial parts of any two wave functions in the DRN, and is given by

$$\Xi_{n'l',nl} = \int_0^\infty R^*_{n'l'} R_{nl} r^2\,\mathrm{d}r, \tag{3}$$

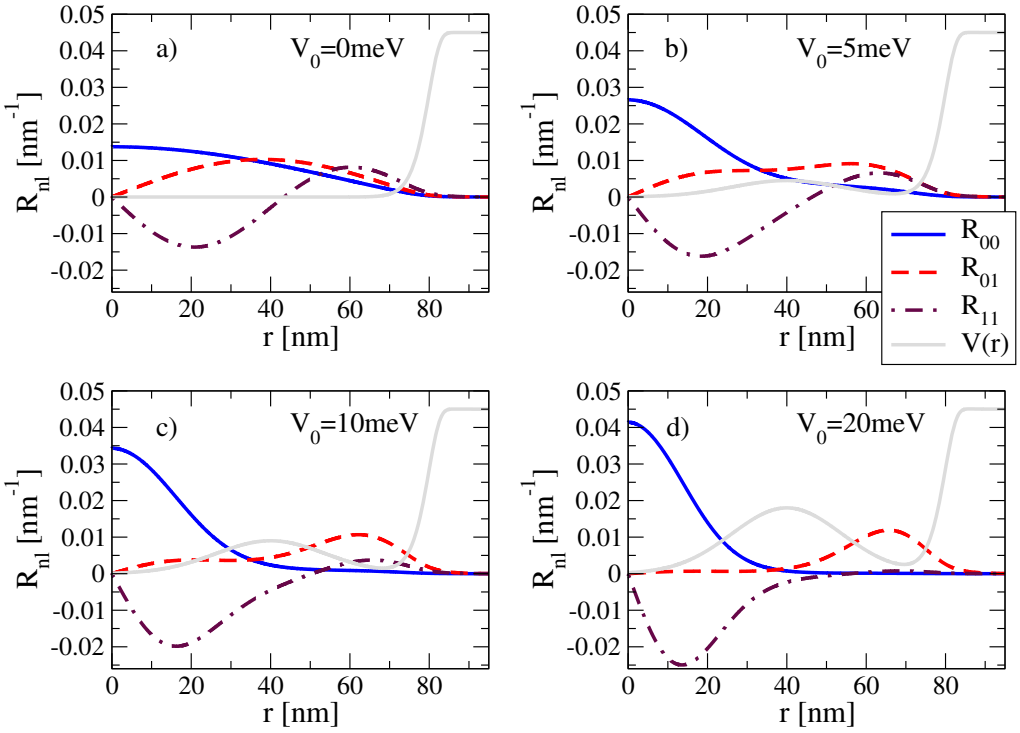


**Figure 4.** The distribution of the wave functions of the three lowest energy states involved in spin relaxation for different values of $V_0$. $V_{QD} = V_{QR} = 0$ meV and $V_1 = 50$ meV is assumed.

where $n'l'$ and $nl$ are the quantum numbers of the two energy states involved in the process under investigation. In the following, we consider a DRN occupied by a *single* electron which couples to photonic (optical absorption) or phononic (spin relaxation) degrees of freedom. For such processes the selection rules allow the electron occupying the ground state to transit/scatter to the states with orbital numbers $l = \pm 1$ only. Then, the relevant OF takes the form

$$\Xi_{00,nl} \equiv \Xi_{nl} = \int_0^\infty R_{00}^* R_{nl} r^2 \, \mathrm{d}r, \tag{4}$$

where $R_{00}$ is the radial part of the ground state wave function (2) and $l = \pm 1$. The second important quantity that depends on confinement and strongly affects absorption and relaxation is the energy gap between the excited orbital and the ground state

$$\Delta_{nl} = E_{nl} - E_{00}. \tag{5}$$

The calculated energy levels, modified by electrical gating, will be used in section 3 to estimate the relaxation times for a set of DRNs.

## 3. Spin relaxation times in dot–ring nanostructures (DRNs)

The spin of a *single* electron in a circularly symmetric DRN placed in a static magnetic field $B$ with energy levels split by the Zeeman energy $\Delta_Z = g_s \mu_B B$ provides a natural system suitable as a memory device in spintronics and as a qubit in a quantum computer [17]. If $k_B T \ll \Delta_Z \ll \Delta_{01}$

then the DRN can be well approximated as a two-level system. The evident goal is to optimize material properties and nanostructure design to achieve long relaxation (and decoherence) times so that sufficient room is left for implementing protocols for spin manipulations and read out.

In our model calculations we assume the in-plane magnetic field $B = 1\,\mathrm{T}$ (the in-plane orientation is favorable as it does not reduce the distance between the orbital states), thus the Zeeman splitting is equal to $\Delta_Z = 0.046\,\mathrm{meV}$.

It was shown both theoretically [18, 19] and experimentally [5, 20, 21] that the most important spin relaxation mechanism in magnetic fields of the order of a few Tesla is spin–orbit (SO) mediated spin–piezoelectric phonon interaction. The extensive discussion of the relaxation times in QDs and QRs has been also given in [22]. In all these studies it was shown that relaxation times increase strongly with the decrease of the nanostructure radius, so we will not consider this aspect here. We rather focus on the change of $T_1$ governed by the change of the confinement potential that defines the investigated DRN structure.

The formula for the relaxation time $T_1$ governed by the Dresselhaus SO interaction is given by (for detailed derivation see [18]):

$$\frac{1}{T_1} = \frac{\Delta_Z^5}{\eta}\left(\sum_{n,l}\frac{\Xi_{nl}^2}{\Delta_{nl}}\right)^2, \tag{6}$$

$$\eta = \frac{\hbar^5}{\Lambda_p(2\pi)^4(m^*)^2}. \tag{7}$$

$\Lambda_p$ is the dimensionless constant depending on the strength of the effective spin–piezoelectric phonon coupling and the magnitude of SO interaction, $\Lambda_p = 0.007$ for GaAs type systems [18, 21]. For a given quantum number $n$ the orbital states with $l$ and $-l$ are degenerated (in a parallel magnetic field), so we take into account only positive values of $l$ multiplying the relevant quantities by a factor of 2. We have checked that for a single electron the relaxation time is determined by the SO coupling to (at most) two lowest excited orbital levels allowed by the selection rules $n = 0$, $l = 1$, thus

$$\frac{1}{T_1} = \frac{4\Delta_z^5}{\eta}\left(\Gamma^{01} + \Gamma^{11}\right)^2, \tag{8}$$

where

$$\Gamma^{01} = \frac{\Xi_{01}^2}{\Delta_{01}}, \quad \Gamma^{11} = \frac{\Xi_{11}^2}{\Delta_{11}}. \tag{9}$$

The quantities entering $T_1$ depend on the potential confining the electrons which determines the orbital energy spectrum, the shape of the orbital wave functions and therefore the OF.

Let us first consider a limiting case when $V_{QD} = V_0 = 0$. Then a DRN is a circular QD with radius $r_0 = 80\,\mathrm{nm}$. The calculated quantities are collected in table 1 (first row) and the corresponding wave functions are presented in figure 4(a). The results show that $T_1$ is entirely determined by the virtual excitation to the first excited orbital state and the reason of small $T_1$ is the relatively large $\Xi_{01}$. The second allowed excited state ($n = 1$, $l = 1$) lies too far in energy to let the electron scatter and the symmetry of the wave function (the dot-dashed line in figure 4(a)) causes a small value of $\Xi_{11}$. Thus this state does not contribute. It is also seen in figure 5(c) where the relaxation times, calculated independently for transitions 00–01 ($T_1^{01}$) and 00–11 ($T_1^{11}$), are plotted. The resulting relaxation time of the nanostructure $T_1$ (dot-dashed solid

**Table 1.** The values of $\Delta_{nl}$, $\Xi_{nl}$, $T_1$ and $\sigma_{i,f}$ as a function of the height of the barrier $V_0$. The parameters are: $r_{\mathrm{QD}} = 25$ nm, $r_{\mathrm{barrier}} = 40$ nm, $r_{\mathrm{QR}} = 70$ nm, $V_{\mathrm{QD}} = V_{\mathrm{QR}} = 0$ meV and $V_1 = 50$ meV.

| $V_0$ | $\Delta_{01}$ (meV) | $\Delta_{11}$ (meV) | $\Xi_{01}$ (nm) | $\Xi_{11}$ (nm) | $T_1$ (ms) | $\sigma_{01}$ (nm$^2$) | $\sigma_{11}$ (nm$^2$) |
|---|---|---|---|---|---|---|---|
| 0 | 0.807 | 3.91 | 5.87 | 0.45 | 0.05 | 6.12 | 0.175 |
| 5 | 1.48 | 3.61 | 3.74 | 1.45 | 0.9 | 4.55 | 1.66 |
| 10 | 2.29 | 4.30 | 1.47 | 2.34 | 18 | 1.1 | 5.16 |
| 15 | 2.85 | 5.26 | 0.53 | 2.30 | 74.2 | 0.18 | 6.13 |
| 20 | 3.26 | 6.12 | 0.20 | 2.16 | 151 | 0.03 | 6.29 |

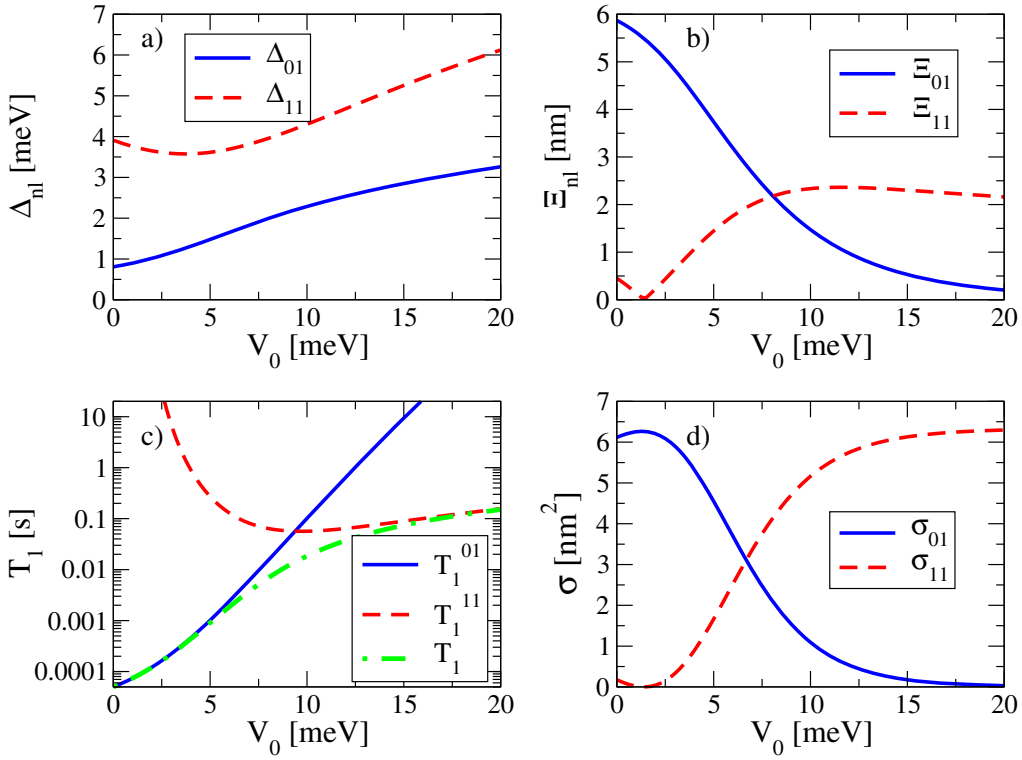


**Figure 5.** The dependence of the orbital gaps $\Delta_{nl}$ (a), OFs $\Xi_{nl}$ (b), relaxation times (c) and photon absorption cross section (d) on the height of the potential $V_0$. Other parameters ($V_{\mathrm{QD}}$, $V_{\mathrm{QR}}$ and $V_1$) are the same as in figure 4. The dot-dashed green line shows the overall relaxation time of the DRN, whereas blue and red lines represent individual relaxation times for phonon coupling to the $R_{01}$ and $R_{11}$ states, respectively.

green line in figure 5(c)) for $V_0 = 0$ overlaps with $T_1^{01}$. The small value of $T_1$ in this case results from the large radius of the considered QD.

To get longer $T_1$ small OFs are required and therefore one should take into account a nanostructure in which the wave functions of the ground and first excited orbital states will be separated so that $\Xi_{01}$ will be very small (while keeping $\Delta_{01}$ reasonably large). It can be done by introducing to a QD a circular potential barrier. When the barrier $V_0$ is present, the

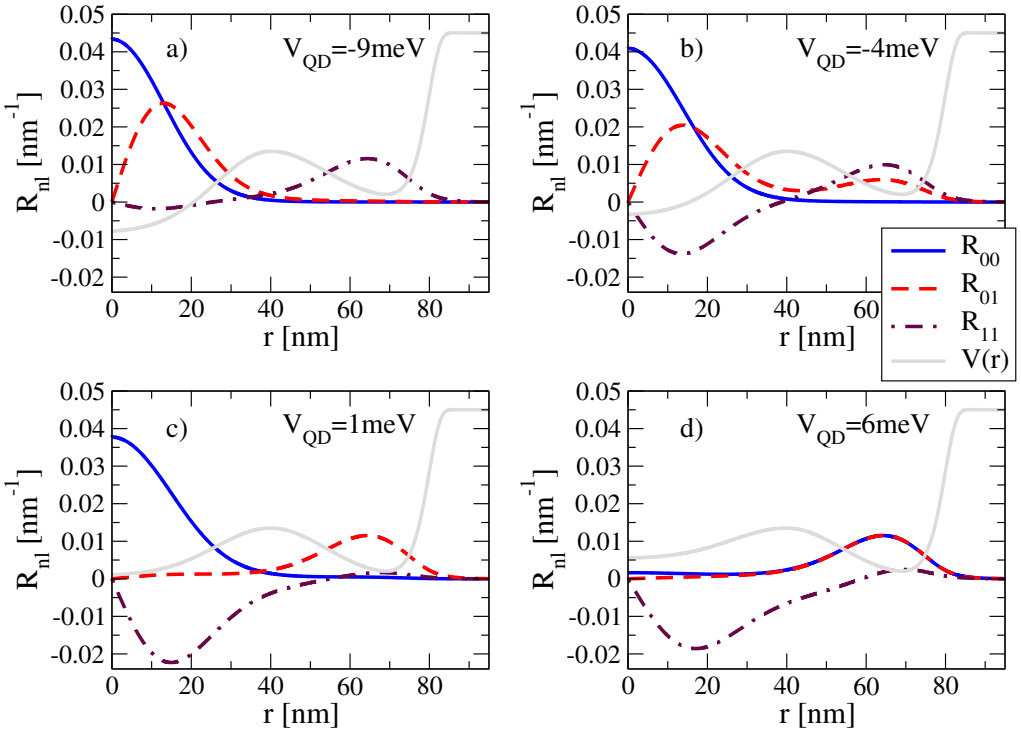


**Figure 6.** The distribution of the wave functions of the first three energy states and for different values of $V_{\mathrm{QD}}$. $V_0 = 15$ meV and $V_1 = 50$ meV is assumed.

structure divides, forming the DRN and the wave function distribution changes drastically (figures 4(b)–(d)). In figures 5(a) and (b), we plotted $\Delta_{nl}$ and $\Xi_{nl}$ respectively as a function of $V_0$, the values are given in table 1. Comparing these figures we see that, in contrast to $\Xi_{nl}$, $\Delta_{nl}$ changes very little with $V_0$ and it is $\Xi_{nl}$ which determines $T_1$. Indeed, when $\Xi_{nl}$ increases then $T_1^{nl}$ decreases and vice versa. For small $V_0$ the dominant contribution to relaxation is given by the state $E_{01}$ (figure 5(c)). With increasing $V_0$ the wave function of $E_{01}$ moves over to QR which results in a decrease of $\Xi_{01}$ (increase of $T_1^{01}$) with a simultaneous increase of $\Xi_{11}$ (decrease of $T_1^{11}$). For $V_0 \approx 9$ meV the contributions to $T_1$ from $E_{01}$ and $E_{11}$ are equal and by further increasing the height of the barrier it becomes the *higher* excited state ($E_{11}$) that determines $T_1$—a rather unusual situation. A similar effect, recently obtained experimentally by changing the shape of the QD by electrical gating [5], also resulted in an increase of $T_1$ by about an order of magnitude.

To summarize this part, we have shown that by changing the barrier height one can change considerably the relaxation time of DRN by manipulating the orbital energy states and their wave functions.

Similar considerations can be done for DRNs by changing, instead of the barrier height, the potential well offset $V_{\mathrm{QD}}$. Such manipulations can be done experimentally by the application of a disk-shaped potential gate below the QD. For such a setup one can move individual wave functions between the QD and QR (figures 6(a)–(d)) and for sufficiently large values of $V_{\mathrm{QD}}$ (positive or negative) we can model the geometry of the nanostructure from QD through DRN to QR. The possible applications of these features will be given in section 5. The results of the calculations of relevant $\Delta$s and $\Xi$s are presented in figure 7 and the corresponding relaxation

**Table 2.** The values of $\Delta_{nl}$, $\Xi_{nl}$, $T_1$ and $\sigma_{i,f}$ as a function of $V_{QD}$. The parameters are : $r_{QD} = 25$ nm, $r_{barrier} = 40$ nm, $r_{QR} = 70$ nm, $V_0 = 15$ meV, $V_{QR} = 0$ meV and $V_1 = 50$ meV.

| $V_{QD}$ | $\Delta_{01}$ (meV) | $\Delta_{11}$ (meV) | $\Xi_{01}$ (nm) | $\Xi_{11}$ (nm) | $T_1$ (ms) | $\sigma_{01}$ (nm$^2$) | $\sigma_{11}$ (nm$^2$) |
|---|---|---|---|---|---|---|---|
| −9 | 6.73 | 10.3 | 2.07 | 0.03 | 240 | 6.33 | 0.002 |
| −5 | 6.1 | 7 | 2.14 | 0.34 | 150 | 6.15 | 0.18 |
| −2 | 4.45 | 5.65 | 0.54 | 2.20 | 106 | 0.29 | 6.03 |
| 0 | 2.85 | 5.26 | 0.53 | 2.30 | 74.2 | 0.17 | 6.12 |
| 3 | 0.51 | 4.64 | 3.20 | 2.16 | 0.21 | 1.14 | 4.76 |
| 9 | 0.15 | 6.98 | 10.1 | 0.71 | $2 \times 10^{-4}$ | 3.36 | 0.78 |

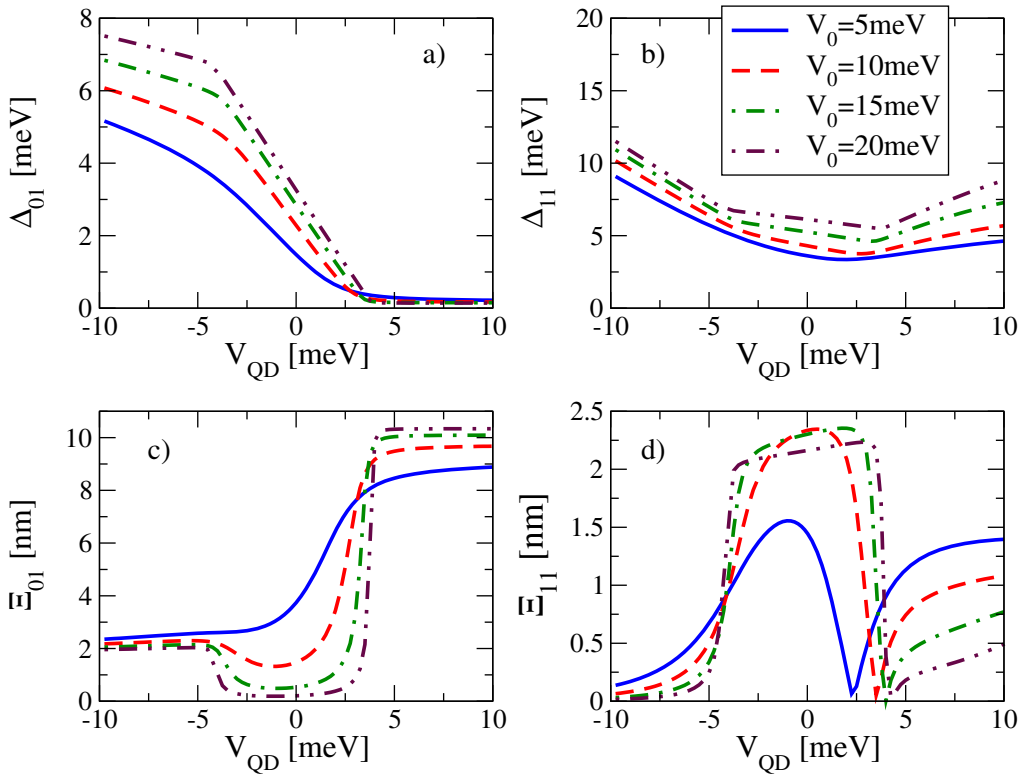


**Figure 7.** Dependence of the orbital energy gap $\Delta_{nl}$ (panels (a) and (b)) and OF $\Xi$ (panels (c) and (d)) to the first (panels (a) and (c)) and second (panels (b) and (d)) excited states as a function of $V_{QD}$ for different values of $V_0$.

times are given in table 2. We see that within this method one can change $T_1$ in the same range as when manipulating $V_0$ (see $T_1$ in tables 1 and 2).

The increase of $T_1$ is possible even in the limiting case of $V_0 = 0$, i.e. if we manipulate only $V_{QD}$. It is shown in figures 8(a) and (b) with the resulting relaxation times. This seems to be the simplest possible method to increase $T_1$ by introducing a small disk-shaped gate below a central part of a big QD (without the separating barrier).

One should stress that the important feature of such studies is not only the value of $T_1$ itself but the possibility to change it by external conditions which can be steered by electric fields.

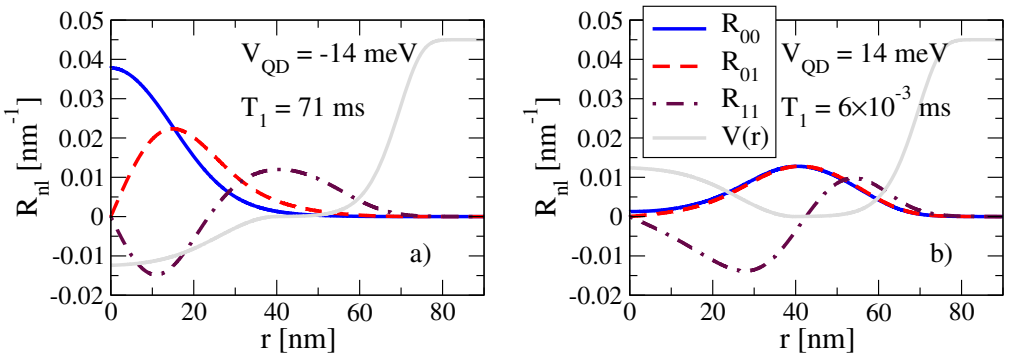


**Figure 8.** Distribution of the radial parts of the electron wave function and the corresponding relaxation time for (a) $V_{\mathrm{QD}} = -14$ meV, (b) $V_{\mathrm{QD}} = 14$ meV.

Besides these long relaxation times have been obtained taking into account only SO mediated interaction with piezoelectric phonons. However other mechanisms of relaxation, (e.g. due to fluctuations of the electric and magnetic field, deformational phonons, multiphonon processes and circuit noise) which we neglected in the above model calculations, can further limit the relaxation time.

In the next section, we discuss another quantity which is determined by the DRN parameters, namely the intraband absorption of microwave and infrared radiation.

## 4. Engineering the optical absorption of DRNs

The cross section for photon absorption due to electron transition from the $i$th bound state $E_i(n_i, l_i)$ to the $f$th bound state $E_f(n_f, l_f)$ in the dipole approximation is given by the formula [23–25]

$$\sigma_{i,f} = \frac{16\pi^2\beta\hbar\omega\Xi_{i,f}^2}{n_2}\delta(E_f - E_i - \hbar\omega)F_{\mathrm{FD}}(E_i, E_f), \tag{10}$$

where $\beta = 1/137$ is the fine structure constant, $l_f = l_i \pm 1$, $n_2$ is the refractive index and $F_{\mathrm{FD}}(E_i, E_f) \equiv f_{\mathrm{FD}}(E_i) - f_{\mathrm{FD}}(E_f)$, with $f_{\mathrm{FD}}(E)$ being the Fermi–Dirac distribution function. In these considerations we assume $B = 0$ and $k_{\mathrm{B}}T \ll \Delta_{01}$. Replacing the delta function by the Lorentzian function with half-width $\Gamma$ and neglecting the influence of temperature we obtain the maximum cross section at the resonance frequency

$$\sigma_{i,f}^{m} = \frac{16\pi^2\beta\,\Xi_{i,f}^2}{n_2\Gamma}\Delta_{i,f}. \tag{11}$$

With the help of (11) one can analyze the frequency selective absorption for a range of initial and final states. For concreteness we calculate the absorption coefficient from the orbital ground state $E_{00}$ to the first excited orbital state $E_{01}$ at frequency $\omega_{01}$ ($\hbar\omega_{01} \simeq \Delta_{01}$) and to the second excited state $E_{11}$ at frequency $\omega_{11}$ ($\hbar\omega_{11} \simeq \Delta_{11}$) and show how it can be modified for different DRNs. Then (11) can be written as

$$\sigma_{00,n1}^{m} = \sigma_{n1} = \frac{16\pi^2\beta\Delta_{n1}\Xi_{n1}^2}{n_2}, \quad n = 0, 1 \tag{12}$$

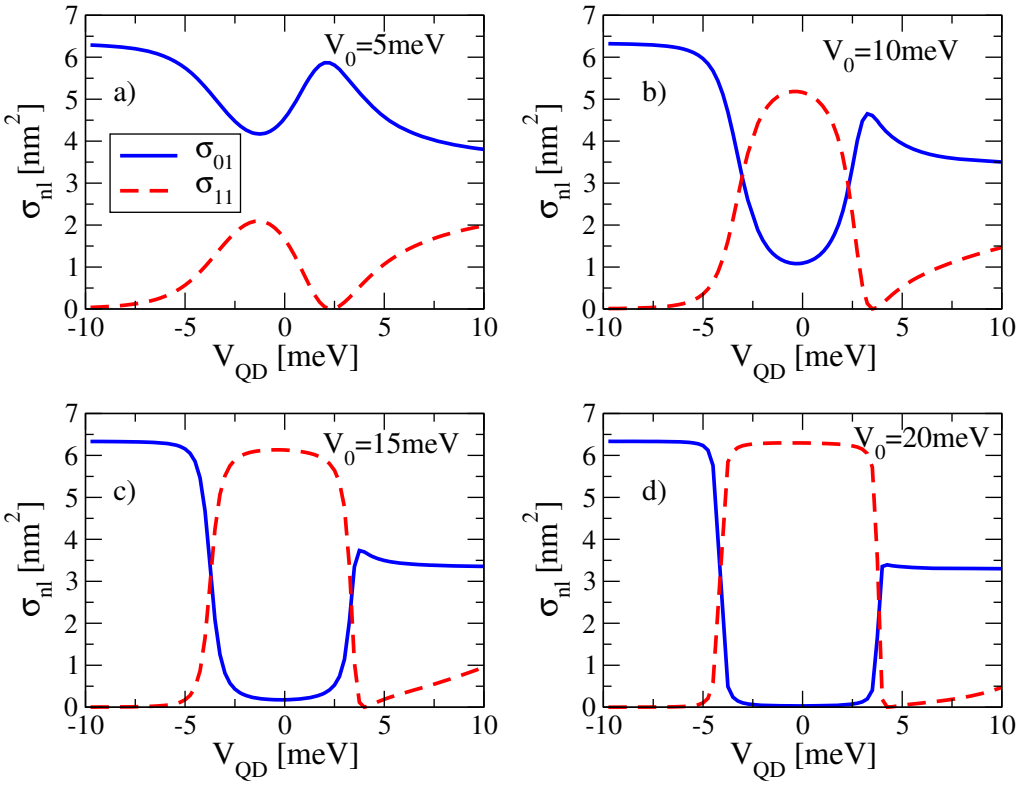


**Figure 9.** Photon absorption cross section for transition from the ground state to the first (solid blue line) and the second (red dashed line) states as a function of $V_{QD}$ for different values of $V_0$.

(assuming $\Gamma = 1$ meV, $n_2 = 3.25$). The absorption cross sections for the first two optical transitions as a function of the barrier height $V_0$ is shown in figure 5(d). Manipulating $V_0$ we can utilize the *on*/*off* switching for absorption of a photon of frequency $\Delta_{01}/\hbar$ ($\Delta_{11}/\hbar$). The ratio between *on* and *off* cross sections is about 40 (see the last two columns in table 1).

The optical absorption strongly depends also on $V_{QD}$ (figures 9(a)–(d)) for sufficiently large $V_0$. For $V_{QD}$ located much below $V_{QR}$ the wave functions of the ground and first excited state lie in the QD and that of the second excited state in the QR (see e.g. figure 6(a)). It results in a high (small) absorption cross section $\sigma_{01}$ ($\sigma_{11}$). With decreasing the potential well offset for $V_{QD}$ around –3 meV the distribution of the wave functions changes considerably resulting in $\sigma_{11}$ much bigger than $\sigma_{01}$. By further increasing $V_{QD}$ the wave functions $R_{00}$, $R_{01}$ move over to QR and $R_{11}$ stays in QD (see e.g. figure 6(d)) which results in a reversed situation. For small $V_0$ these effects are much weaker.

These considerations allow us to engineer the DRNs according to their applications:

(i) one can design DRNs to get the most effective absorption required for efficient infrared and microwave photodetectors, or

(ii) one can design DRNs with negligible absorption at $\hbar\omega_{01}$ or $\hbar\omega_{11}$, i.e. structures which will be transparent for the respective photon frequency.

**Figure 10.** Electron wave functions in an array of DRNs in the case when electrons are located in the QDs (left panel) and in the QRs (right panel).

By changing $V_{QD}$ one can smoothly move over from highly absorbing to almost transparent DRNs. The absorbed photon energy can be changed to a large extent by changing the radius of DRN, the barrier height and the material (e.g. for the structure with $m^* = 0.04m_e$ it changes from microwave to far infrared).

## 5. The conducting properties of arrays of DRNs

Apart from the unique properties of a single DRN, interesting behaviour emerges when such structures are combined into a two-dimensional array. If they are located sufficiently close to each other, electrons can tunnel from one DRN to another one, making a system that resembles a narrow band crystal. The tunnelling rate depends on the overlap of the electron wave functions on adjoining structures. And since we are able to control the shape of the wave functions, we can control the overlap, and thereby manipulate the transport properties of the crystal-like structure. If the electron wave functions are located in the QDs, the overlap is effectively zero and the system behaves like an insulator. On the other hand, when the wave functions are located in the QRs, the overlap is much larger which results in metallic character. These two situations are illustrated in figure 10.

Since the electronic correlations are not taken into account in our approach, we do not expect a true metal–insulator transition. However, in real nanosystems the Coulomb blockade is present and when the number of electrons per DRN is exactly one (the half-filled case) a Mott-type transition can occur [26]. Then, by changing the gate voltage we would be able to induce the metal–insulator transition. In a finite system, even in the presence of Coulomb correlations, it will not be a phase transition, rather a crossover behaviour between states with localized and itinerant electrons. Such a transition results in a change of the conductance of the array of DRNs. This effect does not require an array consisting of a large number of DRNs: even a single DRN coupled to two leads should have a different conductance depending on the relative position of the bottoms of the QR and QD confining potentials. In the case of two adjoining DRNs the system can be effectively described as a double QD with the coupling controlled by the shape of the confining potential. The conductance of such a system as a function of the inter-dot tunnelling rate has been studied, e.g. in [27]. Similarly, in the case of one-dimensional and two-dimensional arrays of QD the conductance has been studied in [28] and [29], respectively. Note, that in all these systems the Coulomb correlations play an important role.

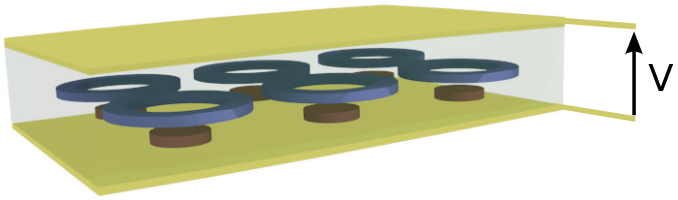


**Figure 11.** Example of a spatial configuration of QR and QD that allows for controlling $V_{\mathrm{QR}}$ and $V_{\mathrm{QD}}$ by an external electrostatic field.

If we assume that there is a tunnelling between adjoining QRs, but not between adjoining QDs, the array of DRNs can be described by a periodic Anderson-like Hamiltonian [30]

$$\mathcal{H} = \sum_{\langle i,j\rangle\sigma} (t_{ij} - \epsilon_{\mathrm{QR}}\delta_{ij}) c^{\dagger}_{i\sigma} c_{j\sigma} - \epsilon_{\mathrm{QD}} \sum_{i\sigma} f^{\dagger}_{i\sigma} f_{j\sigma} + V \sum_{i\sigma} (f^{\dagger}_{i\sigma} c_{i\sigma} + \mathrm{h.c.}) + \frac{U_{\mathrm{QD}}}{2} \sum_{i} n_i (n_i - 1), \tag{13}$$

where $c^{\dagger}_{i\sigma}$ ($f^{\dagger}_{i\sigma}$) creates an electron in the $i$th QR (QD), $t_{ij}$ is the transfer energy between adjoining QRs, $V$ describes the hybridisation between states in QD and QR at the same site. In accordance with the Coulomb blockade picture the interaction between electrons in a given QD can be parameterized by a capacitive charging energy $U_{\mathrm{QD}} = e^2/C$. Coulomb interaction in QRs is neglected. The difference of the atomic levels $\epsilon_{\mathrm{QD}} - \epsilon_{\mathrm{QR}}$ can be controlled by the voltage applied to the QD's gates.

There is also another possibility to induce the metal–insulator transition. When a random gate voltage is applied to DRNs an on-diagonal disorder is introduced into the array and the Anderson localization is expected. Controlling individual DRNs in an array may be involved since it requires a supply of voltage to every gate. However, if we are interested only in the global properties of such an array, there is no need to control individual DRNs. In order to be able to control all the DRNs in the same way, i.e. to force electrons to occupy QDs or QRs in all nanostructures, we can place the QDs in one layer and the QRs in another one, located above (or below) the first layer. Then, the difference $\epsilon_{\mathrm{QD}} - \epsilon_{\mathrm{QR}}$ is proportional to the strength of electric field applied to the whole array perpendicularly to the layers. Such configuration is shown in figure 11. Of course, since in this case QDs and QRs are vertically separated, one can use sufficiently large QDs instead of QRs.

A similar approach has been proposed by Ugajin [31], where an array of coupled QDs was subjected to an external electric field. The QDs were of a convex shape and the applied field moved electrons into the convex portion which led to a larger barrier width between adjacent dots and a smaller transfer energy.

## 6. Summary

The ability to control the quantum state of a single electron is at the heart of many developments, e.g. in spintronics and quantum computing. In contrast to real atoms, quantum nanostructures allow flexible control over the confinement potential which gives rise to wave function engineering.

In our model calculations we have shown that by manipulating the confinement parameters we can alter the overlap of the electron wave functions so that the transition probability will be enhanced or suppressed on demand. We performed systematic studies of the influence of such manipulations on relaxation times, optical absorption and the conducting properties of DRNs. Thus the basic issues of quantum mechanics can be explored to design new semiconductor devices in which specific properties can be optimized.

The wavelength range of the absorption spectra may be largely expanded from microwave to infra-red by utilizing DRNs of different sizes and different materials. The macroscopic variables such as relaxation time, optical absorption or conductivity can be modified by changing on demand the microscopic features of the nanosystem such as the shape and distribution of the wave functions. Combined quantum structures are highly relevant to new technologies in which the control and manipulations of electron spin and wave functions play an important role. To name a few possible applications, one can imagine tunable or switchable microwave waveguides built with the help of arrays of DRNs with variable optical properties or a single electron transistor based on a single DRN coupled to source and drain leads.

The results indicate a novel opportunity to tune the performance of nanostructures and to optimize their specific properties by means of sophisticated structural design.

## Acknowledgments

MMM and MK acknowledge support from the Foundation for Polish Science under the TEAM program for the years 2011–4. EZ acknowledges support from the Ministry of Science and Higher Education (Poland) under grant no. N N202 052940. The authors thank Jerzy Wróbel and Bartłomiej Szafran for valuable discussions.

## References

[1] Hanson R and Awschalom D D 2008 *Nature* **453** 1043
[2] Hanson R, Kouwenhoven L P, Petta J R, Tarucha S and Vandersypen L M K 2007 *Rev. Mod. Phys.* **79** 1217
[3] Somaschini C, Bietti S, Sanguinetti N and Koguchi S 2011 *Nanotechnology* **22** 185602
Sanguinetti S, Somaschini C, Bietti S and Koguchi N 2011 *Nanomater. Nanotechnol.* **1** 14
[4] Shorubalko I, Pfund A, Leturcq R, Borgstörm M T, Gramm F, Müller E, Gini E and Ensslin K 2007 *Nanotechnology* **18** 044014
[5] Amasha S, MacLean K, Iuliana P, Zumbühl D M, Kastner M A, Hanson M P and Gossard A C 2008 *Phys. Rev. Lett.* **100** 046803
[6] Wang Y Y and Wu M W 2006 *Phys. Rev.* B **74** 165312
Raith M, Stano P and Fabian J 2011 *Phys. Rev.* B **83** 195318
[7] Ford C J B, Barnes C H W, Anderson D, Jones G A C, Farrer I, Ritchie D A, McNeil R P G and Kataoka M 2011 *Nature* **477** 439
Elzerman J M, Hanson R, Greidanus J S, Willems van Beveren L H, De Franceschi S, Vandersypen L M K, Tarucha A and Kouwenhoven L P 2003 *Phys. Rev.* B **67** 161308
[8] Silva L G G V D da, Villas-Bôas J M and Ulloa S E 2007 *Phys. Rev.* B **76** 155306
[9] Ning Z, Tian H, Oin H, Zhang Q, Agren H, Sun L and Fu Y 2010 *J. Phys. Chem.* C **114** 15184
[10] For a review see Viefers S, Koskinen P, Singha Deo P and Manninen M 2004 *Physica* E **21** 1
[11] Zhitenev N B, Brodsky M, Ashoori R C, Pfeiffer L N and West K W 1999 *Science* **285** 715
[12] Szafran B, Peeters F M and Bednarek S 2004 *Phys. Rev.* B **70** 125310
[13] Fuhrer A, Lscher S, Ihn T, Henzel T, Ensslin K, Wegscheider W and Bichler M 2001 *Nature* **413** 822

[14] Mano T, Kuroda T, Mitsuishi K, Yamagiwa M, Guo X-J, Furuya K, Sakoda K and Koguchi N 2007 *J. Cryst. Growth* **301** 740
Kuroda T, Mano T, Ochiai T, Sanguinetti S, Sakoda K, Kido G and Koguchi N 2005 *Phys. Rev.* B **72** 20530
[15] Ciurla M, Adamowski J, Szafran B and Bednarek S 2002 *Physica* E **15** 261
[16] Lis K, Bednarek S, Szafran B and Adamowski J 2003 *Physica* E **17** 494
[17] Żak R A, Röthlisberger B, Chesi S and Loss D 2010 *Riv. Nuovo Cimento* **33** 7
[18] Khaetskii A V and Nazarov Y V 2001 *Phys. Rev.* B **64** 125316
[19] Golovach V N, Khaetskii A V and Loss D 2004 *Phys. Rev. Lett.* **93** 016601
[20] Heiss D, Jovanov V, Klotz F, Rudolph D, Bichler M, Abstreiter G, Brandt M S and Finley J J 2010 *Phys. Rev.* B **82** 245316
[21] Kroutvar M, Ducommun Y, Heiss D, Bichler M, Schuh D, Abstreiter G and Finley J J 2004 *Nature* **432** 81
[22] Zipper E, Kurpas M, Sadowski J and Maśka M M 2011 *J. Phys.: Condens. Matter* **23** 115302
[23] Milanovic V and Ikonic Z 1989 *Phys. Rev.* B **39** 7982
[24] Halonen V, Pietiläinen P and Chakraborty T 1996 *Europhys. Lett.* **33** 377
[25] Bondarenko V and Zhao Y 2003 *J. Phys.: Condens. Matter* **15** 1377
[26] Stafford C A and Das Sarma S 1994 *Phys. Rev. Lett.* **72** 3590
[27] Sztenkiel D and Świerowicz R 2007 *Acta Phys. Pol.* **111** 361
Fransson J and Eriksson O 2004 *Phys. Rev.* B **70** 085301
Ziegler R, Bruder C and Schoeller H 2000 *Phys. Rev.* B **62** 1961
[28] Shangguan W Z, Au Yeung T C, Yu Y B and Kam C H 2001 *Phys. Rev.* B **63** 235323
[29] Chen H, Wu J, Li Z-Q and Kawazoe Y 1997 *Phys. Rev.* B **55** 1578
[30] Anderson P W 1961 *Phys. Rev.* **124** 41
[31] Ugajin R 1994 *J. Appl. Phys.* **76** 2833
Ugajin R 1996 *Phys. Rev.* B **53** 10141